View metadata, citation and similar papers at core.ac.uk
brought to you by CORE
provided by Online Publishing @ NISCAIR

Indian Journal of Chemical Technology
Vol. 26, November 2019, pp. 473-482

Thermodynamic and kinetic study of CO_2 adsorption/desorptionon amine-functionalized sorbents

Yamin Liu*[1, 2], Junjie Wu[1], Chengbiao Zhang[1], Yilan Chen[1], Min Xiong[1], Ronghui Shi[1], Xiaoying Lin[1] & Xiaojing Yu[1]

[1]School of Ecological Environment and Urban Construction, Fujian University of Technology, Fuzhou 350118, Fujian, China

[2]Fujian Indoor Environment Engineering Technology Research Center, Fuzhou 350118, Fujian, China

E-mail : mingjing2000@126.com

Received 23 March 2018; accepted 20 August 2019

The thermodynamic and kinetic characteristics of CO_2 adsorption of SBA-16 loaded with pentaethylenehexamine (PEHA) have been investigated using adsorption column system. The Langmuir isotherm model fitts the CO_2 adsorption isotherms well, and the average isosteric heat of adsorption is 59.6 kJ/mol, indicating that the CO_2 adsorption on PEHA-loaded SBA-16 is chemisorption. The Avrami fractional dynamics model is very suitable for illustrating the adsorption behaviour of CO_2 adsorption, and the results of kinetic analysis show that increasing the partial pressure of CO_2 or the working temperature is beneficial to the adsorption of CO_2. Three desorption methods were evaluatedto achieve the optimal desorption method. The results show that VTSA and steam stripping method are effective methods for industrial CO_2 desorption. Steam stripping may be more suitable for plants that already have low-cost steam. The activation energy E_a of CO_2 adsorption/desorption is calculated using Arrhenius equation. The activation energy E_a of CO_2 adsorption/desorption was calculated using the Arrhenius equation. The results show that the absolute value of E_a (adsorption) decreases with the increase of CO_2 partial pressure. In addition, the E_a value of vacuum rotary regeneration method and steam stripping method is smaller than the E_a value of temperature swing regeneration.

Keywords: Thermodynamic, Kinetic, CO_2, Adsorption, Desorption

It is widely believed that the global warming iscaused by the anthropogenic emissions of greenhouse gases (GHG)[1]. CO_2 is one of the major greenhouse gases, and a large amount of the man-made CO_2 is believed to be the main cause of global warming. The current CO_2 level in the atmosphere is around 400 ppm[2], much higher than the upper safe limit of 350 ppm[3]. As CO_2 is an inherent product of fossil fuel combustion, the increase in CO_2 emissions recorded in the last decades is mainly related to power generation, transportation, and industrial processes. Today, about 85% of the world's energy needs come from fossil fuels[4, 5]. In the future, fossil energy may remain the most important resource for energy supply in both developed and developing countries[6]. Some estimates of the world's energy landscape suggest that by 2100, fossil fuels will still account for more than 65% of total energy output[7]. Under this energy structure, the wide application of CCS(CO_2 capture and storage) technology may be an important part of the lowest cost energy system that achieves the long-term goal of significantly reducing anthropogenic CO_2 emissions[7–10].

CCS technology includes three methods: pre-combustion capture, post-combustion capture and oxy-fuel combustion[11]. Among them, the post-combustion capture technology has a cost competitive advantage over the other two technologies, and is the main choice for the power and industrial sectors to decarbonize. The post-combustion capture technology mainly includes liquid ammonia absorption, porous materials adsorption, and membrane purification. Among these technologies, the porous materials adsorption technology has drawn wide attention in recent years due to its potential to meet the requirements of energy-efficient and cost effective CO_2 remediation[11]. And lots of research groups around the world have been working to develop new solid adsorbents[12, 13], such as zeolites molecular sieve[14,15], mesoporous silicon[16–18], metal-organic frameworks (MOFs)[19–22], carbon nanotubes (CNTS)[23–26], and the polymeric amine containing hybrid adsorbents[27–30].

Rapid adsorption/desorption is the key to the practicality of the CO_2 adsorption process during industrial operations. The faster the CO_2 adsorption/ desorption, the better the economics of CCS technology[31]. So, ideal solid adsorbent for industrial CO_2 capture applications should not only have a large CO_2 adsorption capacity and highly CO_2 selectivity, but also have a high CO_2 adsorption / desorption rate[32] , and have a long service life. Furthermore, the determination of the isosteric adsorption heat is an important aspect that

characterized the potential of adsorbents for gas adsorption. However, so far, studies on the adsorption thermodynamics and kinetics of CO_2 adsorption/ desorption by amine loaded solid adsorbent are not enough.

In our previous work[33], we found that the PEHA loaded SBA-16 exhibited favorable CO_2 adsorption/ desorption performance under simulated flue gas conditions, such as desirable selectivity, high CO_2 adsorption capacity and recyclability.

In this work, we further investigated the adsorption thermodynamics and kinetics of CO_2 adsorption/ desorption by PEHA loaded SBA-16. Caurie[34] equation was used to calculate the isosteric adsorption heat of CO_2 adsorption onto PEHA loaded SBA-16. Two rationalized kinetic models regarding adsorbent-adsorbate interactions, the intracrystalline diffusion equation and Avrami's model, were selected to investigate the kinetics of CO_2 adsorption onto PEHA loaded SBA-16.The optimal desorption method was obtained by comparing three kinds of desorption methods for the regeneration of adsorbent. Meanwhile the Avrami's model was selected to describe desorption kinetics.

Experimental Section

Synthesis of PEHA-loaded SBA-16

The solidsorbent for CO_2 capture was prepared by impregnating SBA-16 into PEHA solution, and the sample was noted as SP-30, here 30 represented the weight percentage of PEHA in the composites. Detailed preparation program were described in our previous study[33].

Adsorption experiments

CO_2 adsorption experiments were carried out according to previously reported method[33]. A detail step can be seen in the Supplementary Files (SF). Here 2.0 g of SP-30 was treated in a 100 cm^3/min N_2 (99.99%) stream at 383 K for 1h and then cooled to the design experimental temperature. Then, a mixed gas (N_2vol. 90% and CO_2vol. 10%) (99.99%) was input. The CO_2 concentration was maintained at 10 vol. % and the pressure was at atmospheric pressure. The CO_2 concentration was measured by a gas chromatograph (GC) on line.

Desorption experiments

The desorption tests were carried out using the CO_2 adsorption column experimental system. The adsorbents should fully adsorb CO_2 before desorption test begins. The concentration of CO_2 in outlet gas was measured by GC on line.

In order to find the best desorption method, temperature swing adsorption combined N_2-stripping (TSA-N_2), vacuum temperature swing adsorption (VTSA) and steam-stripping(SST) were used to regenerate the adsorbent. For TSA-N_2 regeneration, the adsorption column was heated to the design regeneration temperature after the adsorbent fully absorbed CO_2, the inlet of the adsorption column was then switched to a N_2 flow. Meanwhile the concentration of CO_2 in outlet gas was measured by the GC every minute. According to the CO_2 concentration and N_2 flow rate, the total amount of CO_2 was calculated. Therefore, the efficiency of CO_2 desorption could be obtained at a given time.

For VTSA desorption, closed the inlet valve after the adsorption process had reached equilibrium. The outlet of the adsorption column was then connected to a vacuum pump system that could operate under a given pressure. At the same time, the mass of adsorbent which adsorbed enough CO_2 was quickly measured. After that, the adsorption column was rapidly heated to the desired temperature, while the pressure of the adsorption column was controlled by the vacuum pump to the required pressure. The mass of adsorbents was weight every 2 min. Once the mass of regenerated adsorbent was equal to the mass of the initial sample (pure adsorbent), the adsorbents were considered completely regenerated, and the total mass loss equaled to the amount of desorbed CO_2.

The SST tests were carried out according to Li's method[35]. Here, the adsorbents are regenerated by contacting the adsorbents with a 378 K saturated stream,and the steam flow rate was set to 0.12 g / min. In order to measure the desorbed CO_2, N_2 sweep was used after the adsorbent has been desorbed using pure steam(the N_2 purge contacts the mixed CO_2/water stream downstream of the adsorption column). The mixture was then passed through a condenser to remove the water, and then the dry N_2-CO_2 mixture was transported to the GC on line.

Adsorption thermodynamics model

The determination of the (Q_{st}) is an important aspect that characterized the potential of adsorbents for gas adsorption. Isosteric heat of adsorption is commonly defined as the enthalpy change on adsorption. It is a direct indicator of the strength and heterogeneity of the interaction between the adsorptive and the adsorbent. Quantification of the Q_{st} value is very important in kinetic studies of adsorption processes. The heat released upon adsorption will be partly absorbed by the adsorbent. As a result, the adsorbent's temperature will rise and the equilibrium

adsorption rate will change[36]. Generally, Clausius-Cleperon equation is frequently used to calculate the adsorption heat[37]. But this equation is a general thermodynamic equation applicable at low gas pressures to measure the heat of phase transition rather than for calculating the heat of adsorption at high pressures.The heat of adsorption is a measure of the firmness with which adsorbed molecules are held to the adsorbent surface at adsorption centres and not of intermolecular energies[37]. So the use of the Clausius-Cleperon equation as basis for estimating isosteric heat of adsorption may underestimates the adsorption heat[34]. And some scholars have modified the Clausius-Clapeyron equation or deduced a better equation to estimate the heat of adsorption. From the expanded form of his unimolecular adsorption equation, Caurie[34] has derived an alternative equation (Equation 1, Name as Caurie Equation) similar to the Clausius–Clapeyron equation for computing isosteric heat of adsorption from sorption data, and obtained good results. Therefore, the Caurie Equation was selected to calculated the adsorption heat of CO_2 adsorption process.

$$\ln P = -\frac{Q_{st}/2}{R}\cdot\frac{1}{T} + Cons \quad \ldots (1)$$

where P is CO_2 partial pressure (P_a), T is the absolute temperature(K), and R denotes the universal gas constant, 8.314 J/mol/K. For a given q_a, C_0 at multiple temperatures is obtained from adsorption isotherms curve and is subsequently converted to *P*.

Adsorption kinetic models

In order to design the actual adsorption unit and operation parameters, it is necessary to understand the kinetic process of adsorption. By establishing the adsorption kinetic model, the performance of sorbents can be described quantitatively, and the overall mass transfer in the adsorption process can be understood. Researchers have established a number of different adsorption kinetic models to describe different adsorption processes, and it is a commonly way to obtain the best fitting model by fitting the obtained experimental adsorption data with many common models. In this work, two commonly models were used to investigate the kinetics of CO_2 adsorption on SP-30.

Classical intracrystalline diffusion model

Assuming that the mass transfer resistance is controlled by theintracrystalline diffusion and that a crystal of sample may beregarded as an approximately spherical object, the diffusion equationin spherical coordinate is written as equation 2[38, 39],

$$\frac{\partial q}{\partial t} = \frac{1}{r^2}\frac{\partial}{\partial r}\left(r^2 D_c \frac{\partial q}{\partial r}\right) \quad \ldots (2)$$

where D_c denote as the intracrystalline diffusitivity and $q(r, t)$ represents the adsorbed amount at time t and radial position r. If the uptake of gas by the adsorbent is small relative to the total amount introduced into the system, the initial boundary and conditions can be givenas equation 3:

$$q(r,0) = q_0^{'}, q(r_c,0) = q_0\ , \left(\frac{\partial q}{\partial r}\right)_{r=0} = 0 \quad \ldots (3)$$

The solution of equation 3 is given byequation 4,

$$\frac{\bar{q} - q_0^{'}}{q_0 - q_0^{'}} = \frac{m_t}{m_\infty} = 1 - \frac{6}{\pi^2}\sum_{n=1}^{\infty}\frac{1}{n^2} exp\left(-\frac{n^2\pi^2 D_c t}{r_c^2}\right) \quad \ldots (4)$$

where $\bar{q}$ is the average adsorption amount in the particle, q_0' represents theinitial adsorption amount in the particle, q_0 is the equilibriumuptake in the particle, and m_t/m_∞ is the fractional adsorptionuptake.

At short times, equation 4 is approximated byequation 5,

$$\frac{m_t}{m_\infty} = \frac{6}{\sqrt{\pi}}\sqrt{\frac{D_c}{r_c^2}t} - 3\frac{D_c}{r_c^2}t, \quad \ldots (5)$$

This expression is accurate to within 1% for $m_t/m_\infty < 0.85$ (or$D_c/r_c^2 < 0.4$). In this study, equation 5 was used as the diffusion modelequation to regress the adsorption kinetic data, and the diffusiontime constant ($D_c/r_c^2, 1/S,$) can be obtained.

Avrami's fractional-order kinetics model:The Avrami's model was based on the Avrami equation, and was originally applied for particle nucleation[40]. Recently, people began to use this model to simulate the phase changes and crystal growth of materials[41], or to explore the dynamic adsorption behavior of surface amine-functional adsorbents[32,42]. The model is commonly expressed asequation 6,

$$\frac{dq_t}{dt} = k_a^n t^{n-1}(q_e - q_t) \quad \ldots (6)$$

where k_α is the kinetic constant of the Avrami model, and n denotes the Avrami exponent, which is often in fractional form, and reflects possible mechanism changes in the adsorption process[43]. In fact, the term n reflects the dimensions of the growth of absorbed species at the adsorption site, where n = 2 represents one-dimensional growth, n = 3 two-dimensional growth,

and so on[44]. For uniform adsorption, i.e., where the probabilities of adsorption in any zone within a fixed time interval are equal, $n = 1$[40,45]. If $n = 2$, the adsorption process, beginning from the adsorption point on the adsorbent surface, is a perfect one-dimensional growth that is continuously formed and has a constant rate[44]. The fractional order of this model originate from the complication of the reaction mechanism or the simultaneous occurrence of multiple reaction paths[41,46]. Thus, Avrami's fractional-order model is well suited for analyzing adsorption kinetics data, and for explaining the mechanism of CO_2 adsorption [47]. The integrated form of Equation6isequation 7,

$$q_t = q_e[1-e^{-(k_a t)^n}] \quad \ldots (7)$$

Desorption kinetic models

In order to further investigate the above-mentioned CO_2 desorption methods, some desorption kinetic model should beused to describe the kinetic process of the above-mentioned CO_2desorption methods. Kinefuchi *et al.*[48] discovered that Avrami's model could fit the regeneration process well. Given the advantages of Avrami's fractional-order model, Avrami's fractional-order model was chosen in this work. In order to study the regeneration process, the Equation 7 is changed to Equation 8:

$$y = 1-e^{-(k_a t)^n} \quad \ldots (8)$$

where y corresponds to the proportion of desorption.

Results and Discussion

Isosteric Heat of the Adsorption

The adsorption isotherms for CO_2 adsorption onSP-30 at various temperatures (293, 303, 313, 323, 333, and 343 K) are presented (Fig 1). The adsorption

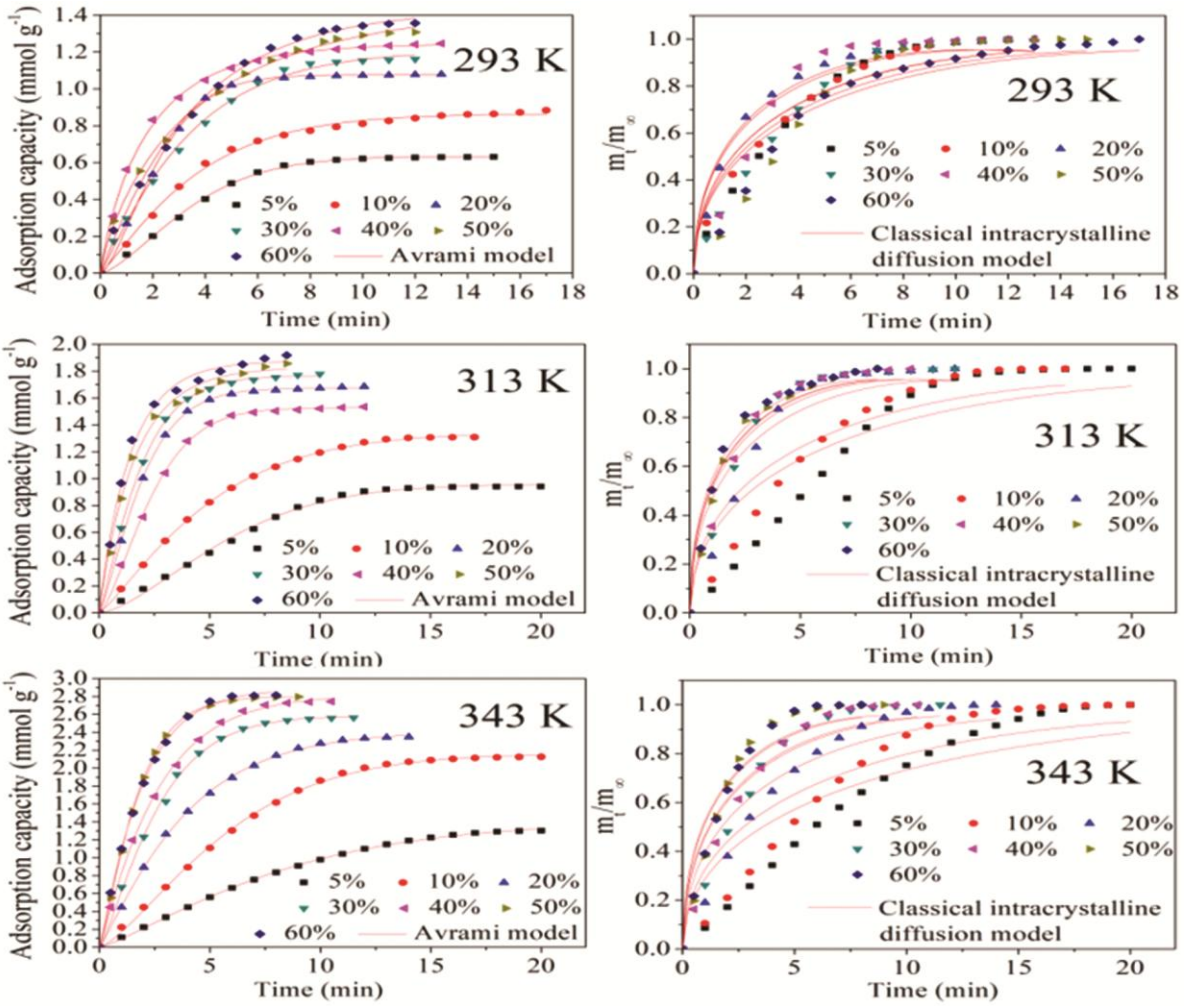

Fig. 1 — Comparison of the results of adsorption kinetics models and the experimental CO_2 uptakes of SP-30 at various CO_2 partial pressurefor various adsorption temperatures.

Table 1 — Parameter values of Langmuir model based on fitting to CO_2 adsorption isotherms for SP-30 at various temperatures and the Q_{st} values obtained by Caurie equation.

q_a (mmol/g)	0.6	0.8	1	1.2	1.4	1.6	1.8	2
R^2	0.991	0.989	0.980	0.992	0.996	0.981	0.978	0.990
Slope	2295.4	2668.9	3220.9	3729.5	3895.3	3929.6	4301.3	4650.7
Q_{st}(KJ/mol)	−38.2	−44.4	−53.6	−62.0	−64.8	−65.3	−71.5	−77.3

isothermsare fitted with the Langmuir model, and the fitting parameters are presented in Table 1. It can be observed that the R^2 is in the range of 0.978 to 0.996, which means that the Langmuir isotherm model fits the CO_2 adsorption isotherms well.

The regression lines of *lnP* versus *1/T* under various q_a were seen. The Q_{st} values of SP-30 at 293-343 K for constant q_a of 0.6-2.0 mmol/g (in 0.2 mmol/g increments) are then determined from the slopes of the regression lines, and the Q_{st} values are also presented in Table 1. The Q_{st} values are negative, implying that the entropy isreduced in the adsorption process. This is consistent with the exothermic character of the adsorption process. The average isosteric heat of adsorption is 59.6 kJ/mol, this value is higher than the value of the enthalpies of physical-sorption (below 40 kJ/mol).High enthalpies indicate that the interaction between CO_2 molecule and adsorbent surface groups is strong, so the CO_2 adsorption on SP-30 ischemisorption.

Adsorption kinetics

The isothermal adsorption testes at different CO_2 partial pressure(i.e., 5, 10, 20, 30, 40, 50, and 60 vol%)and at different temperatures (i.e., 293, 303, 313, 323, 333, and 343 K) were carried out to investigated the kinetics of CO_2 adsorption on SP-30. The experimental data were simulated using two absorption kinetics models introduced in Subsection 2.5. The fitted curves are also shown in Fig. 1. The approximated values of the model parameters and corresponding coefficients of determination R^2 are listed in the Table. According to the R^2 values, we note that the Classicalintracrystalline diffusion model cannot fit the experimental data well, the fitting $R^2$is between 0.841 and 0.977. This results mean that the CO_2 adsorption on SP-30 is not micropore diffusion process, because this model is often used to simulate the micropore diffusion and has good consistency with experimental data.

Base on the R^2 values, we find that Avrami's model presents the best description for the adsorption behavior of CO_2 adsorption on SP-30, its R^2 value is between 0.994-0.999. This result shows that Avrami's model is well suited for analyzing CO_2 adsorption kinetics data, and for explaining the mechanism of CO_2 adsorption on SP-30. This also means that the CO_2 adsorption on SP-30 process is chemisorption process, which is consistent with the conclusion of section 3.1.

k_a increases with increasing temperature. The high viscosity of PEHA at low temperature is adverse to the diffusion of CO_2 into the SP-30 pore, resulting in small k_a. At high temperature, the viscosity of PEHA decreases, so a large number of active sites in the pores can react with CO_2, resulting in the increase of k_a. The k_a rise with rising CO_2 concentration, confirming that highCO_2 partial pressure promotes CO_2 diffusion into pores to contact with the reaction active sites.

The obtained Avrami exponent *n* is between 1 and 2, indicating that the adsorption rate decreases gradually with the one-dimensional growth of the adsorbed nuclei[44,49]. The reason maybe that the initial adsorption of CO_2 on uniformly exposed surface is likely to be homogeneous, additional adsorption may be formed nearthe CO_2 adsorption sites after completion of the initial adsorption, leading to the deviations in the consistency of CO_2 adsorption sites and a value of *n* greater than 1[44].

The term *n* is related to the existence of a different adsorption mechanism[50]. Small changes in *n* at different temperatures indicate that the adsorption mechanism is similar in the experimental temperature range.

As described before, k_a is dependent on temperature, and can be calculated by the following equation (Arrhenius equation),

$$k_a = Ae^{-(E_a/RT)} \quad \text{... (9)}$$

where *A* is the Arrhenius pre-exponential factor which is assumed to be independent of temperature, E_a is the apparent activation energy, and *R* denote as the universal ideal gas constant. A plot of lnk_a versus 1/*T* is shown in Figure 2.

From the fitting lines, activation energy (E_a) andpre-exponential factor (*A*) can be calculated based

on the slope and intercept. The values of A and E_a calculated through linear regression are listed in Table 2. Table 2 shows that the value of E_a decreases with increasing C_0, indicating that a high CO_2 partial pressure promotes the adsorption of CO_2. The E_a obtained by this work are similar to other studies. Serna-Guerrero reported that the E_a of CO_2 adsorption on TRI-PE-MCM-41 was 1.38 kJ/mol. And Wang's research showed that the *Ea* of CO_2 adsorption on MgAl N1, MgAl N2, and MgAl N3 was 11.08, 12.68, and 11.96 kJ/mol for respectively.

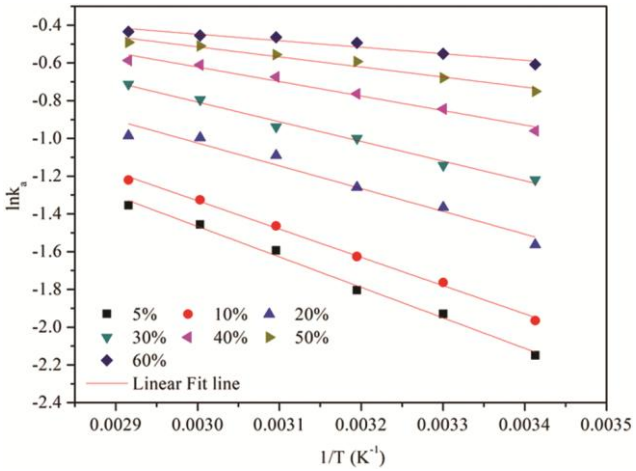

Fig. 2 — Arrhenius plots for the kinetic constants k_a.

CO_2 desorption

TSA-N_2 desorption

The results of TSA-N_2 desorption test are presented in Fig. 3. Obviously, the desorption time decreased with increase of temperature, and the adsorbent cannot be fully regenerated at 363 K. This indicates that the temperature is the main factor in the desorption of CO_2 due to the chemical interaction between the adsorbent and the surface group. The experimental results also showed that the higher nitrogen flow was favorable to the desorption of CO_2, and the higher the nitrogen flow rate was, the shorter the desorption time was. However, when the flow rate increased to a certain value (for this experiment was 100 mL/min), the increase of N_2 flow rate did not significantly shorten the time of desorption.

VTSA desorption

Figure 4 shows the experimental results of CO_2VTS Adesorption under various temperature and pressure. Same with the results of TSA-N_2 test,

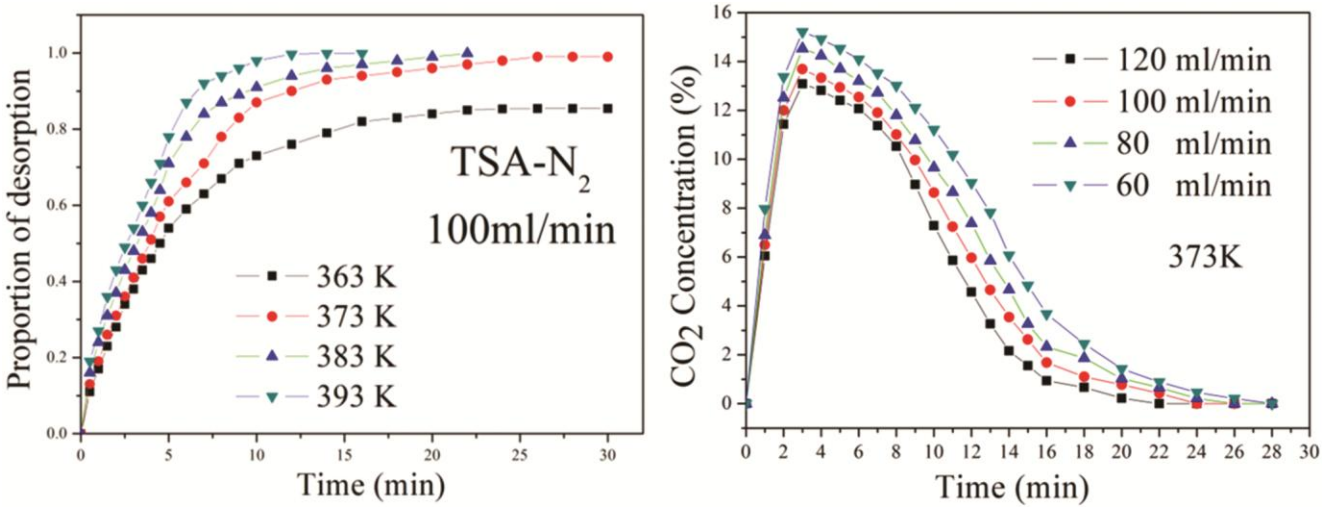

Fig. 3 — Results of TSA-N_2 desorption experiments

Table 2 — Arrhenius parameters calculated from the experimental CO_2 adsorption isotherms fitted to the Arrhenius equation.

CO_2 concentration (vol%)	A (1/s)	*Ea* (kJ/mol)	R^2
5	0.000131	13.421	0.991
10	0.000427	12.455	0.997
20	0.002104	10.032	0.990
30	0.015036	8.662	0.981
40	0.024383	6.384	0.989
50	0.040315	4.438	0.976
60	0.046767	2.871	0.999

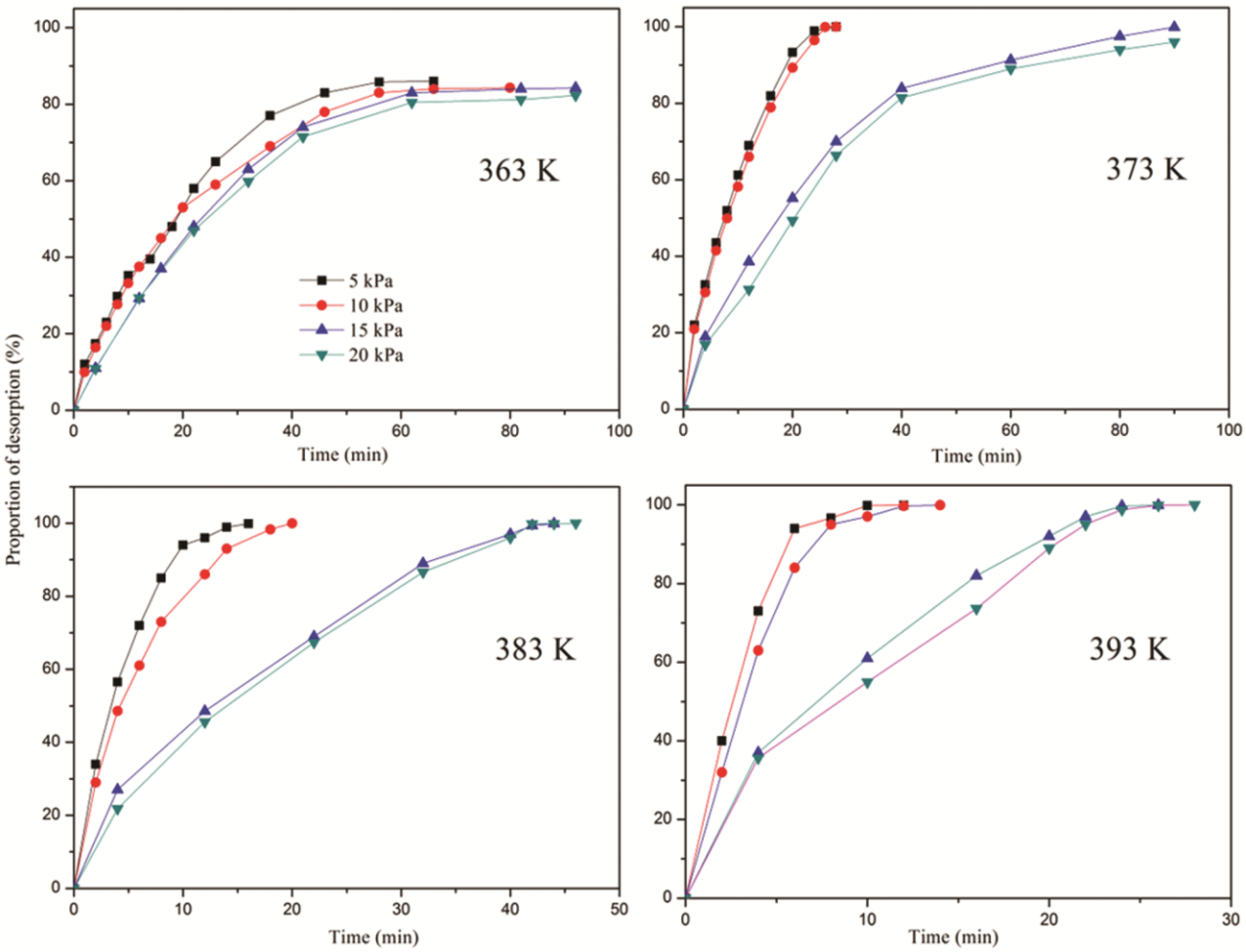

Fig. 4 — Results of VTSA desorption tests

the adsorbent cannot be fully regenerated at 363 K. At constant temperature, the desorption time decreases with the decrease of adsorption column pressure. When the temperature is over 373 K, the increase of temperature can significantly reduce the totaldesorption time under the same pressure.Based on the results of the experiments, we note that good desorption could be achieved under following two conditions:①Pressure is 10KPa and T = 393 K. ②Pressure is 5 KPa and T = 383 K.

SST desorption

The SST experimental results of CO_2 desorption under different temperature and steam flow rate are represented in Fig. 5. Like TSA-N_2 and VTSA desorption, temperature is the key factor of CO_2 desorption, and the increase of temperature can reduce the total desorption time.With the increase of steam flow rate, the totaldesorption time decreased gradually. However, when the flow rate was greater than 0.10 g/min, there was no significant change in the desorption time. So, the optimal SST condition may be T = 378 K and steam flow rate is 0.10 g/min.

Stability of adsorbent in the cyclic adsorption/desorption tests

Adsorbent may be destroyed during the desorption, so the stability of adsorbent is very important for practical use. For SST, it is easy to think that when the steam heat passed on to the adsorbent, some of the steam condenses on the surface of the adsorbent[51], because of the lack of covalent bond between amine and carrier, as well as amine easily dissolved in water, some amine will be washed away during the steam stripping, this will lead to a decrease in adsorption capacity.

In order to investigate the stability of SP-30 during the desorption, 10 cyclic adsorption/desorption tests were conducted for each desorption method (adsorption at 343 K, 10 vol. % CO_2), and the results are shown in Fig. 6. The conditions of the desorption experimentare as follows: ①TSA-N_2, T = 383 K, flow rate is 100 ml/min; ②VTSA, T = 383 K, pressure is 5 KPa; ③SST, T = 378 K, steam flow rate is 0.10 g/min.

Table 3 — Kinetic parameters of the Avrami's fractional-order modelbased on fitting to experimental CO_2 desorption data for SP-30 at various temperatures.

	VTSA	VTSA	VTSA	VTSA	TSA-N_2	TSA-N_2	TSA-N_2	TSA-N_2	Steam	Steam	Steam
T (K)	363	373	383	393	363	373	383	393	378	388	398
k_a(1/min)	0.056	0.095	0.165	0.254	0.022	0.045	0.081	0.164	0.144	0.239	0.342
n_A	1.309	1.618	1.346	1.111	0.823	0.983	1.025	1.062	1.160	1.137	1.203
R^2	0.984	0.994	0.994	0.997	0.997	0.996	0.997	0.986	0.997	0.997	0.994

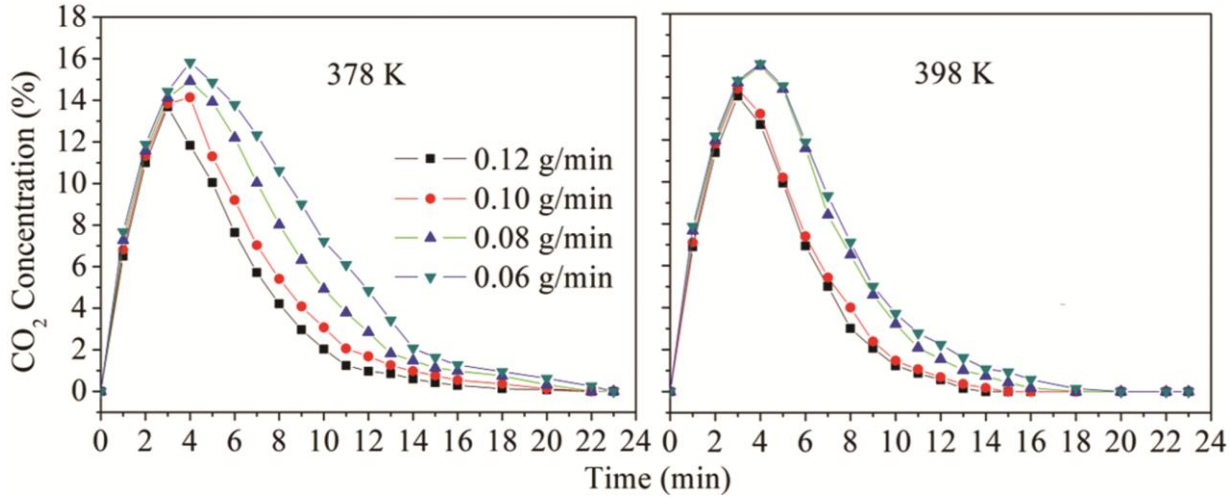

Fig. 5 — Results of SST desorption experiments

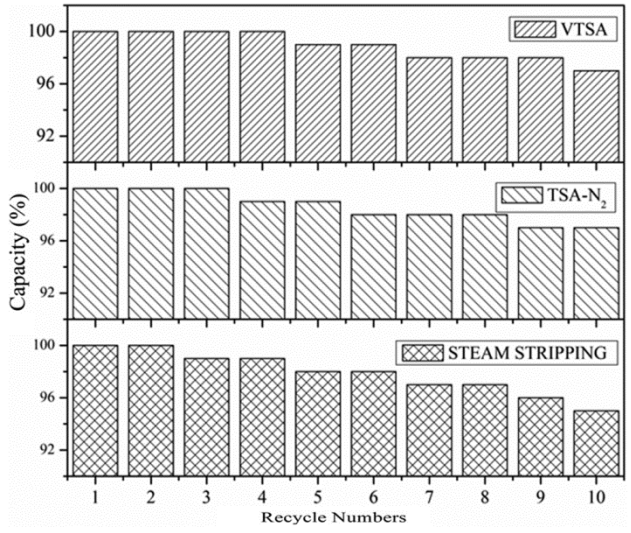

Fig. 6 — Recycle adsorption/desorptiontests of SP-30(Adsorption at 343 K, CO_2: 10 vol.%, N_2: 90 vol.%, gas flowrate: 100 mL/min.Desorption: ①VTSA, T = 383 K, pressure is 5 KPa; ② TSA-N_2, T = 383 K, N_2 flow rate is 100 mL/min; ③SST, T = 378 K, steam flow rate is 0.10 g/min. Capacities are normalized to the initial capacity found in the first experiment.).

The cyclical data revealed that the performance of the SP-30 was fairly stable, with only 3-5% drop in the adsorption capacity after 10 adsorption/desorption cycles. Even with the SST method, unlike what we had previously imagined, the adsorption capacity only decreased by 5%. The results of cyclic adsorption/desorption tests clearly showed that all three desorption methods are effective for SP-30 regeneration. However, in the real industry, nitrogen is rarely used as a stripping gas to regenerate adsorbent, mainly to avoid the impurity of CO_2. Although the product gasproduced by SST process contained CO_2 and steam, the vapor is easily converted into a liquid state by compression and condensation and removed from the gas to produce a highly purity CO_2 gas. Furthermore, low-grade, low-cost steam (Saturated steam, about 378 K, is generally considered to be a low-value waste heat, most of which already exists in refinery or power plant, but is not used.) may be sufficient to regenerate the solid sorbent.It is obvious that the product gas obtained by the VTSA method is a high purity CO_2 gas.

In conclusion, the VTSA and SST are promising method for real industry CO_2 desorption. And the SST may be more suitable for factories that already have low-cost, low-cost steam.

Desorption kinetics

Avrami's fractional-order model was used to simulate the desorption process of the above three desorption methods. The Avrami's fractional-order model fitted curves. The parameters and the corresponding R^2 values for the fitted Avrami fractional-order models are presented in Table 3. Three desorption methods were fitted to themodel well.

Table 4 — Parameters calculated from CO_2 desorption isotherms fitted to the Arrhenius equation

	VTSA	TSA-N_2	SST
A (min^{-1})	2.652×10^7	4.804×10^9	4.316×10^6
E_a(kJ·mol)	−60.271	−78.817	−54.036
R^2	0.998	0.998	0.987

The Avrami kinetic constant k_a of VTSA and SST method are greater than that of TSA-N_2 at the same temperature, indicating that these two methods have a faster desorption rate, which was consistent with the experimental result. The k_a value of VTSA is similar to the k_a value of SST at similar T, indicating that the two methods have similar desorption rate. We note that k_a increases with increasing desorption T, indicating that the temperature is the dominant factor for the regeneration of the adsorbent, and higher temperature is benefit to desorption.

The T-dependence of $k_a$can also be described by the Arrhenius equation. A plot of lnk_a versus 1/$T$for CO_2 desorption. The value of A and Ea calculated by nonlinear rregression are presented in Table 4. The absolute value of E_a of VTSA and SST method are smaller than that reported by Sun *et al.*[52], who used TSA-N_2 method (N_2 0.3 L/min at 353 K) and the E_a was −80.79 kJ/mol. The reason may be that, for VTSA, the vacuum pump and heating together provide the energy of CO_2 desorption, and for SST, the steam can transfer the heat directly to the adsorption site.

Conclusion

Thermodynamics and kinetics analysis of CO_2 adsorption onto PEHA-functionalized SBA-16 under various condition are presented in this paper, meanwhile, desorption methods and the relevant desorption kinetics are also investigated. The Langmuir isotherm model fitted the CO_2 adsorption isotherms obtained in this study well, and the average isosteric heat of adsorption is determined to 59.6 kJ/mol, which indicated that the CO_2 adsorption on SP-30 was chemisorption. Compared with the Classical intracrystalline diffusion model, Avrami's model is considered to be more suitable to describe the adsorption behavior of CO_2 adsorption on SP-30. The increase of k_a with rising CO_2 concentration indicate that high CO_2 partial pressure promoted CO_2 diffusion into pores to contact with the reactionactive sites. The decrease of the absolute value of E_a (Calculated from Arrhenius equation) with increase of C_0 also confirmed that a high CO_2 partial pressure promoted the adsorption of CO_2. Through the analysis of three regeneration methods, temperature is considered to be the dominant factor in the desorption process due to the chemical bond between CO_2 and adsorbents. Among three desorption methods, VTSA and SST are promising method for real industry CO_2 desorption. And the SST may be more suitable for factories which already have low-cost steam.The optimum temperature for SST is T= 378 K and steam flow rate is 0.10 g/min. The value of E_a calculated in this work is lower than the value reported elsewhere because of the input of the vacuum pump energy in VTSA method and direct heating of the adsorption site by steam in SST method.

Acknowledgement

The authors gratefully acknowledge the financial support of theNatural Science Foundation of Fujian Province (Grant No. 2019J01774; No. 2017J01673; No. 2017 J01568).

References

1 Dao D S, Yamada H & Yogo K, *Ind Eng Chem Res*, 52 (2013) 13810.
2 Keeling R F, Piper S C, Bollenbacher A F& Walker S J, *Scripps Institution of Oceanography, University of California - San Diego, USA 92093-0244*, (*http://scrippsCO$_2$.ucsd.edu/sites/default/files/data/merged_ice_core/merged_ice_core_yearly.csv*), 2015.
3 Hansen J, Sato M, Kharecha P, Beerling D, Berner R, Masson-Delmotte V, Pagani M , Raymo M, Royer D L & Zachos J C, *Open Atmos Sci J*, 2 (2008) 217.
4 Yang H, Xu Z, Fan M, Gupta R, Slimane R B &Wright I, *J Environ Sci*, 20 (2008) 14.
5 Iea, *CO_2 Emissions from Fuel Combustion Highlights*, Volume 2, 2011.
6 Balasubramanian R & Chowdhury S, *J Mater Chem A*, 3 (2015) 21968.
7 Dowell N Mac, Fennell P S, Shah N & Maitland G C, *Nat Clim Chang*, 7 (2017) 243.
8 Abbasi E, Abbasian J & Arastoopour H, *Powder Technol*, 286 (2015) 616.
9 Li J & Hitch M, *Powder Technol*, 291 (2016) 408.
10 Sharma P, Seong J K, Jung Y H, Choi S H, Park S Do, Yoon Y I I & Baek I H, *Powder Technol*, 219 (2012) 86.
11 Mondal M K, Balsora H K & Varshney P, *Energy*, 46 (2012) 431.
12 Wang J, Huang L, Yang R, Zhang Z, Wu J, Gao Y,Wang Q, O'Hare D & Zhong Z, *Energy Environ Sci*, 7 (2014) 3478.
13 Madden D, Curtin T, Hanrahan J P & Tobin J, *AIChE J*, 2016.

14 Gongda C, *Appl Energy*, 169 (2016) 597.
15 Chen S, Fu Y, Huang Y & Tao Z, *J Porous Mater*, 23 (2016) 713.
16 Ma B, Zhuang L & Chen S, *J Porous Mater*, 23 (2016) 529.
17 Kishor R & Ghoshal AK, *Ind Eng Chem Res*, 56 (20) 2017.
18 Ge S, He X, Zhao J, Duan L, Gu J, Zhang Q & Geng W, *Water Air Soil Pollut*, 228 (2017) 460.
19 Ranjbar M, Taher M A & Sam A, *J Porous Mater*, 23 (2016) 375.
20 Jing Y, Wei L, Wang Y& Yu Y, *Microporous Mesoporous Mater*, 183 (2014) 124.
21 Chen C, Lee Y R & Ahn W S, *J Nanosci Nanotechnol*, 16 (2016) 4291.
22 Granados-Correa F, Bonifacio-Martínez J, Hernández-Mendoza H & Bulbulian S, *Water Air Soil Pollut*, 226 (2015) 281.
23 Creamer A E & Gao B, *Environ Sci Technol*, 50 (2016) 7276.
24 Chiang Y C & Juang R S, *J Taiwan Inst Chem Eng*, 71 (2016).
25 Liu Y, Chen Y, Tian L & Hu R, *J Porous Mater*, 24 (2017) 583.
26 Yi H, Zuo Y, Liu H, Tang X, Zhao S,Wang Z, Gao F & Zhang B, *Water Air Soil Pollut*, 225 (2014) 1965.
27 Quang D V, Dindi A, Rayer A V, Hadri N E1, Abdulkadir A & Abu-Zahra M R M, *Greenh Gases Sci Technol*, 5 (2015) 91.
28 Quang D V, Hadri N El & Abu-zahra M R M, *Esj*, 9 (2013) 82.
29 Ünveren E E, Monkul B Ö, Sarıoğlan Ş, Karademir N & Alper E, *Petroleum*, 3 (2016).
30 Liu S H & Sie W H, *Water Air Soil Pollut*, 227 (2016) 263.
31 Samanta A, Zhao A, Shimizu GKH, Sarkar P & Gupta R, *Ind Eng Chem Res*, 51 (2012) 1438.
32 Serna-Guerrero R & Sayari A, *Chem Eng J*, 161 (2010) 182.
33 Liu Y, Lin X, Wu X, Liu M, Shi R & Yu X, *Powder Technol*, 318 (2017) 186.
34 Caurie M, *Int J Food Sci Technol*, 40 (2005) 283.
35 Li W, Choi S, Drese J, Hornbostel M, Krishnan G, Eisenberger P & Jones C, *Chem Sus Chem*, 3 (2010) 899.
36 Agnihotri S, Rood M J & Rostam-Abadi M, *Carbon N Y*, 43 (2005) 2379.
37 Mulet A, Garcia-Reverter J, Sanjuan R & Bon J, *J Food Sci*, 64 (1999) 64.
38 Ruthven D M, Principles of Adsorption & Adsorption Processes, 56 (1984) 168.
39 Thomas W J & Crittenden B, Adsorption Technology and Design, *Aliment Equipos Y Tecnol*, 1998.
40 Avrami M, *J Chem Phys*, 7 (1939) 1103.
41 Ecn L, Fsc D A, Efs V & Cestari A R, *J Colloid Interface Sci*, 263 (2003) 542.
42 Zhao Y, Ding H & Zhong Q, *Appl Surf Sci*, 258 (2012) 4301–4307.
43 Menezes E W, Lima E C, Royer B, de Souza F E, dos Santos B D, Gregório J R, Costa T M , Gushikem Y & Benvenutti E V, *J Colloid Interface Sci*, 378 (2012) 10.
44 Benedict J B & Coppens P, *J Phys Chem A*, 113 (2009) 3116.
45 Num G, *J Chem Phys*, 9 (1941) 177.
46 Cestari A R, Vieira E F, Vieira G S & Almeida L E, *J Hazard Mater*, 138 (2006) 133.
47 Sernaguerrero R, Da Na E & Sayari A, *Ind Eng Chem Res*, 47 (2008) 9406.
48 Kinefuchi I, Yamaguchi H, Sakiyama Y, Takagi S & Matsumoto Y, *J Chem Phys*, 128 (2008) 164712.
49 Bertmer M, Nieuwendaal R C, Barnes A B & Hayes S E, *J Phys Chem B*, 110 (2006) 6270.
50 Vieira R B & Pastore H O, *Environ Sci Technol*, 48 (2014) 2472.
51 Xu X, Song C, Miller B G & Scaroni AW, *Ind Eng Chem Res*, 44 (2005) 8113.
52 Sun Z, Fan M & Argyle M, *Energy & Fuels*, 25 (2011) 2988.